Cell, Vol. 82, 655–664, August 25, 1995, Copyright © 1995 by Cell Press

Nonclassical Binding of Formylated Peptide in Crystal Structure of the MHC Class Ib Molecule H2-M3

Chyung-Ru Wang,*† A. Raúl Castaño,‡ Per A. Peterson,‡ Clive Slaughter,*§ Kirsten Fischer Lindahl,*§‖ and Johann Deisenhofer*§
*Department of Biochemistry
§Howard Hughes Medical Institute
‖Department of Microbiology
University of Texas Southwestern Medical Center
Dallas, Texas 75235-9050
‡Department of Immunology
Scripps Research Institute
La Jolla, California 92037

Summary

H2-M3 is a class Ib MHC molecule of the mouse with a 10^4-fold preference for binding N-formylated peptides. To elucidate the basis of this unusual specificity, we expressed and crystallized a soluble form of M3 with a formylated nonamer peptide, fMYFINILTL, and determined the structure by X-ray crystallography. M3, refined at 2.1 Å resolution, resembles class Ia MHC molecules in its overall structure, but differs in the peptide-binding groove. The A pocket, which usually accommodates the free N-terminus of a bound peptide, is closed, and the peptide is shifted one residue, such that the P1 side chain is lodged in the B pocket. The formyl group is coordinated by His-9 and a bound water on the floor of the groove.

Introduction

Major histocompatibility complex (MHC) class I molecules bind peptides, derived by intracellular processing of viral, bacterial, or endogenous proteins, and present them on the cell surface to cytotoxic T lymphocytes ($CD8^+$ T cells). Each allelic form of a class I molecule preferentially binds peptides that conform to a particular motif, often defined by the second (P2) or fifth (P5) residue and the last residue (Pω), usually P8 or P9 (Rammensee et al., 1993). The general principles behind this ability to bind a broad, but defined, range of peptides has been revealed by X-ray crystallography of classical MHC class Ia molecules (Bjorkman et al., 1987a; Madden et al., 1992; Matsumura et al., 1992a; Guo et al., 1993).

The structures of three human (Bjorkman et al., 1987b; Saper et al., 1991; Garrett et al., 1989; Madden et al., 1991) and two mouse (Fremont et al., 1992; Zhang et al., 1992; Young et al., 1994) class Ia molecules have been determined, first with a mixture of bound peptides and later with defined peptides (Guo et al., 1992; Silver et al., 1992; Madden et al., 1993). These structures are remarkably similar. The first two domains (α1 and α2) of the MHC protein form a groove with closed ends; each domain contributes half of the β-sheet floor of the groove and an α-helix wall. The N-terminus of the peptide is held at one end of the groove by a hydrogen bond network that involves four highly conserved tyrosines at positions 7, 59, 159, and 171, and the C-terminus is held at the other end by the conserved residues Tyr-84, Thr-143, Lys-146, and Trp-147.

Six pockets, A to F, in the groove have been identified in class Ia structures. These pockets are formed by polymorphic residues of the MHC protein, and they generate the specificity for sequence motifs in the peptide. In the human class Ia molecules HLA-A2 (A2), HLA-Aw68, and HLA-B27, the B pocket under the α1 helix accommodates the second side chain of the peptide; in the mouse molecules H2-K^b (K^b) and H2-D^b (D^b), this pocket is not as pronounced, but a deep pocket D on the β-sheet floor holds the P5 side chain. In all the structures, a deep F pocket on the floor holds the Pω side chain.

Most immune responses by $CD8^+$ T cells involve the class Ia molecules, which are encoded by one to three MHC genes and are distinguished by their high level of expression and polymorphism. Additional MHC class I genes encode nonclassical or class Ib molecules, which are less polymorphic, expressed at lower levels and often with a limited tissue distribution (Stroynowski and Fischer Lindahl, 1994). In humans, at least three such genes are expressed; mice have >50 class Ib genes, of which perhaps half are expressed. At least some of the class Ib proteins can bind peptides (Rötzschke et al., 1993; Joyce et al., 1994) and present them to $CD8^+$ T cells (Aldrich et al., 1994; Castaño et al., 1995). The class Ib molecules may serve a more specialized function than class Ia molecules, and such is clearly the case with H2-M3 (M3) (Wang et al., 1991).

M3 is a class Ib protein encoded at the telomeric end of the mouse MHC; its extracellular domains share the length and most consensus residues with class Ia molecules, and it associates with β2-microglobulin (β_2m), but it has a shorter cytoplasmic tail. M3 was discovered because it presents a polymorphic endogenous peptide, derived from the mitochondrially encoded ND1 protein (Loveland et al., 1990) and named MTF (for maternally transmitted factor), as a minor histocompatibility antigen to $CD8^+$ T cells. M3 can also present antigens derived from the intracellular bacterium Listeria monocytogenes to killer T cells from infected mice (Pamer et al., 1992; Kurlander et al., 1992). M3 has a unique specificity for N-formylated peptides (Shawar et al., 1990), naturally made by prokaryotes and mitochondria. M3 can also bind or present nonformylated peptides, but this requires a 10^4-fold higher peptide concentration (Smith et al., 1994), or P1 must be glycine (Vyas et al., 1992). As long as the N-terminus of the peptide is formylated, M3 can accommodate P1 side chains ranging from alanine to lysine or tyrosine (Vyas et al., 1992). Other anchor motifs have not been identified, except for a general preference for hydrophobic or aromatic amino acids (Miller et al., 1994).

†Present address: Gwen Knapp Center for Lupus and Immunology Research, The University of Chicago, Chicago, Illinois 60637-5420.

We have resorted to X-ray crystallography to understand how M3 achieves its unique specificity. Expression in a permanently transfected Drosophila cell line (Jackson et al., 1992) allowed us to produce sufficient quantities of soluble, truncated M3 heavy chains associated with β_2m. For the peptide, we chose a nonamer of the rat form of ND1 (formyl-MYFINILTL); it cross-reacts strongly with the mouse ND1α or MTFα antigen (Hermel, 1992), which has phenylalanine at P2 (Loveland et al., 1990). The crystal structure of M3, refined to 2.1 Å and described here, revealed a novel mode of peptide binding.

Results and Discussion

Overall Structure of M3 Complex

Crystals of the M3–β_2m–MTF complex are triclinic, with two molecules in the unit cell. The structure was determined by molecular replacement with K^b as a search model (Fremont et al., 1992). Table 1 shows the crystallographic data and refinement statistics, and Figure 1 shows sections of the final electron density map. The model includes residues 1–276 of the M3 heavy chain, β_2m (residues B1–B99), the MTF peptide (residues P1–P9), 372

Table 1. Crystallographic and Refinement Data

Statistics	Measurement
X-ray data	
Resolution (Å)	2.1
Unique reflections ($I > 2\sigma$)	33706
Completeness (%)	70
Completeness in 2.17–2.1 Å shell (%)	43
R merge[a] (%)	7.9
Refinement statistics	
Resolution range (Å)	20 to 2.1
R factor[b] (%)	19.0
Number of residues	768
Number of water molecules	372
Number of nonhydrogen atoms	6670
B factors (Å^2)	
Mean for main chain residues	24.4
Mean for side chain residues	26.5
Rmsd from ideality	
Bond distance (Å)	0.014
Bond angle (degrees)	1.88

[a] R merge = $(\Sigma_{hkl}\Sigma_i | I_{hkl,i} - \langle I\rangle_{hkl}|)/\Sigma_{hkl}\Sigma_i I_{hkl,i}$, where $I_{hkl,i}$ is the i-th measurement of the intensity of the reflection with Miller indices hkl. $\langle I\rangle_{hkl}$ is the average intensity.

[b] R factor = $(\Sigma_{hkl}||F_o| - |F_c||)/\Sigma_{hkl}|F_o|$, where $|F_o|$ and $|F_c|$ are observed and calculated structure factor amplitudes.

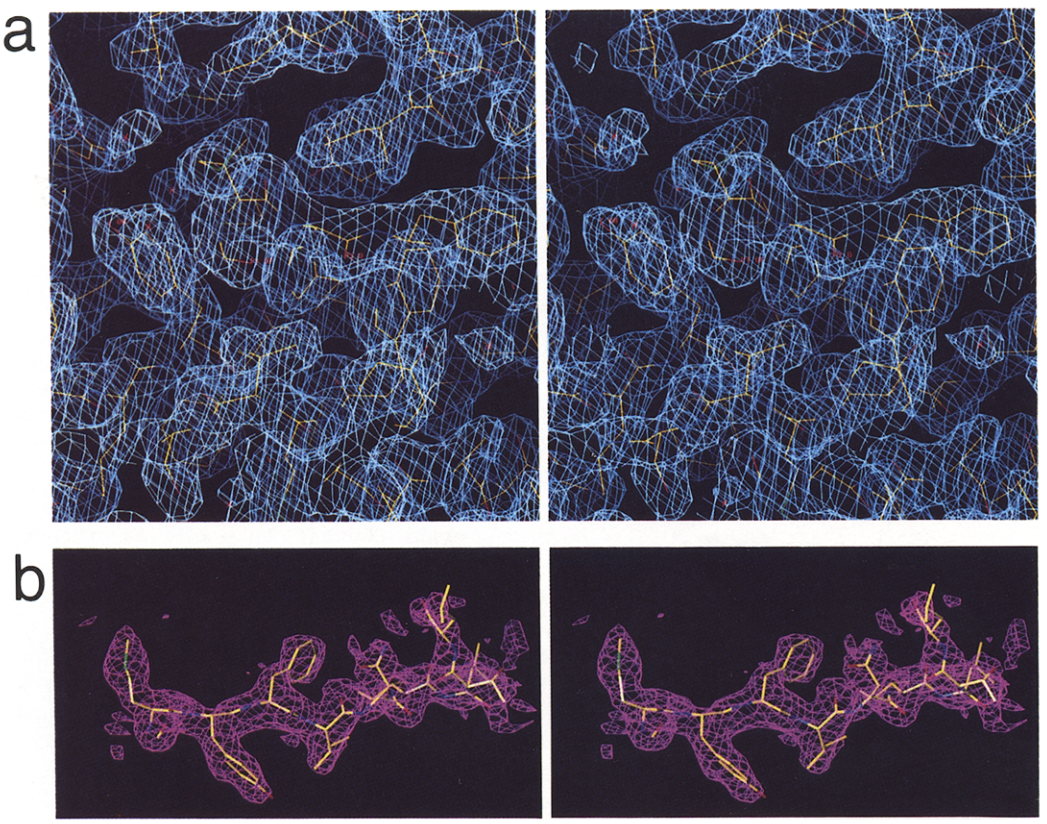

Figure 1. Stereoviews of the Final Electron Density Map

(a) Detailed view near the binding site for the N-formyl group. The electron density map was calculated using 20–2.1 Å diffraction data with model phases and $2F_o–F_c$ as Fourier coefficients. The density is contoured at the 1σ level. Superimposed is the refined model of M3.

(b) Side view of the MTF peptide (fMYFINILTL). Electron density within 1.6 Å of the peptide model is shown at 0.8σ contour level.

water molecules, and one N-acetyl-glucosamine moiety attached to Asn-86 of one of the M3 heavy chains.

All amino acid residues of the M3 heavy chain and β_2m can be unambiguously traced. The electron density in the peptide-binding groove is continuous (Figure 1b), and most of the residues in the MTF peptide have well-defined density; the first three residues have low B factors (~4–40 Å^2), and the rest have B factors similar to the flexible loop regions (~40–80 Å^2). Because the electron density for P9 is not well defined, the conformation of this residue cannot be assigned unambiguously. The histidine tag (His_6) on the M3 heavy chain is disordered. The two molecules in the unit cell are almost identical, except for the regions making crystal contacts; the root-mean-square deviation (rmsd) of all Cα atoms after superposition of the two molecules is 0.29 Å for the M3 heavy chain and 0.31 Å for β_2m.

The overall structure of M3 is similar to MHC class Ia molecules. K^b and A2 were selected for comparison to M3, because their biological function and peptide specificity are well studied, and the structures have been determined to high resolution (Saper et al., 1991; Fremont et al., 1992). Superposition of the α1α2 domains of M3, K^b, and A2 shows that the α3 and β_2m domains are oriented slightly differently in each class I structure (Figure 2a). Table 2 lists the sequence similarity and rmsd of Cα atoms of M3 and other class Ia molecules. Although the sequence of M3 is more similar to mouse than to human class Ia molecules, the structure is not. The relatively large overall rmsd between the M3 and K^b structures is caused by substantial differences in the orientation of individual domains, rather than differences in the polypeptide fold. These differences in domain deposition may reflect the orientation under physiological conditions or could be due to crystal packing.

The rmsd between mouse β_2m in M3 and human β_2m, which are 69% identical in primary sequence, is 0.56 Å for A2 and 0.49 Å for B27, whereas the rmsd for mouse β_2m is 0.86 Å between M3 and K^b and 0.53 Å between M3 and D^b, despite identical primary sequence (Table 2). β_2m in M3 and K^b differ most in residues B52–B54 and the C-terminus. As in human β_2m, residues B52–B54 of β_2m in M3 form a β bulge and break the S4 β strand, which is continuous in K^b (B50–B56). Main chain atoms deviate by >4.5 Å between M3 and K^b in this region. The conformation of numerous side chains also differ between β_2m of M3 and K^b, including B6, B8, B12–B13, B19, B29, B44–B45, B48, B53–B54, B58, B62–B63, B81, and B83. Because many of these changes lie within regions that form the interface with the α1α2 and α3 domains, they affect these interactions profoundly. Of 13 hydrogen bonds between the α3 domain and β_2m in M3, 11 are present in A2, but only five are shared with K^b; of eight hydrogen bonds between the α1α2 domain and β_2m of M3, all are conserved in A2, but only three are present in K^b (Table 3). The main chain conformation of β_2m in D^b is more similar to M3 than K^b, including residues B52–B54 and the C-terminus, and only six side chains differ in conformation between D^b and M3. The interdomain salt bridge between Asp-B53 and Arg-35 in M3 is also present in HLA structures but absent in mouse K^b and D^b. Thus, although the contact areas between heavy chain and β_2m are similar in size and location for all the class I molecules, the different heavy chains cause structural changes in β_2m.

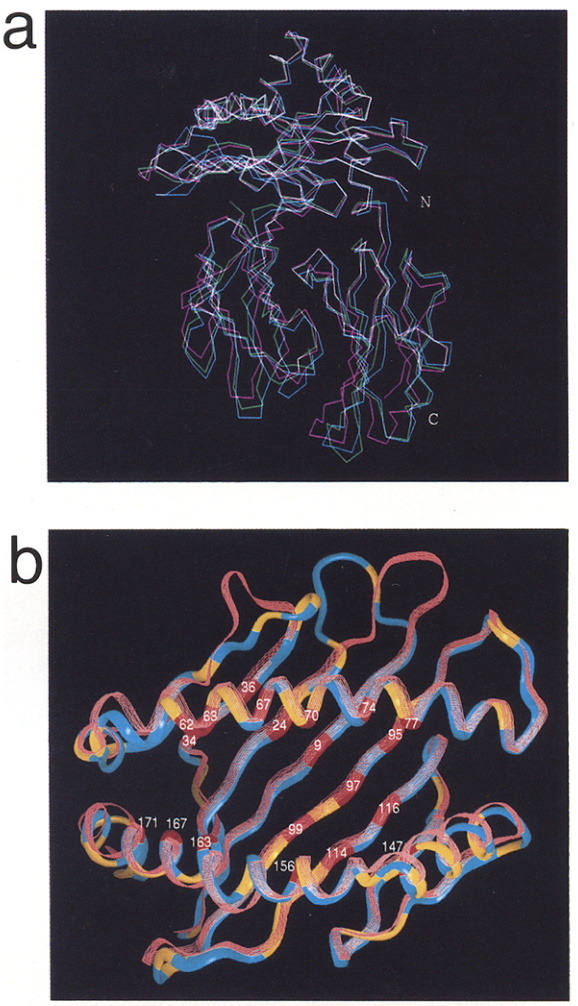

Figure 2. Superpositions of M3 on Class Ia Structures

(a) The Cα traces of M3 (cyan), K^b (magenta), and A2 (green) were obtained by superimposing the Cα coordinates of the α1α2 domains on M3, using the program O.

(b) Comparison of the superimposed α1α2 domains of M3 (cyan) and K^b (pink); 58 residues that differ between the two molecules are marked, with those that point into the groove shown as red and numbered and the others shown as yellow.

In the α1α2 domain, M3 differs most from other class I molecules in two loops, one connecting S1 to S2 (residues 13–21) and the other connecting S3 to S4 (residues 38–45) (Figure 2b), which also differ between K^b and D^b (Fremont et al., 1992; Young et al., 1994). The changes are greater by far in M3, and the likely reason is the loss of three salt bridges, Arg-14–Asp-39, Arg-21–Asp-37, and Arg-44–Glu-61, that otherwise stabilize the loops. In M3, residue 39 is isoleucine, residue 21 is glutamine, and residue 61 is arginine. Strand S4 is extended by four residues in M3 (42–45), and the Cα atom positions deviate up to

Table 2. Comparison of Sequence Similarity and Rmsd of Cα Atoms between M3 and Other Class I Molecules

	M3/K^b		M3/D^b		M3/A2		K^b/D^b		K^b/A2	
Domain	Percent	Ångstrom	Percent	Ångstrom	Percent	Ångstrom	Percent	Ångstrom	Percent	Ångstrom
α1 and α2	61	0.988	58	1.072	61	1.167	85	0.807	71	0.721
α3	76	0.669	81	1.107	72	0.787	92	0.963	72	0.896
β_2m	100	0.864	100	0.530	69	0.556	100	0.896	69	0.832
Overall	75	1.491	75	0.978	66	1.104	90	1.494	71	1.357

Coordinates with the entry numbers 1vaa (K^b), 1hoc (D^b), and 1hhj (A2) were obtained from the Brookhaven Protein Data Bank. Residues 15–20 and 39–43 (the deviating loops of α1) were excluded from the superposition of M3 on the other class I molecules.

10 Å from K^b in both loops. Another significant shift in M3 is in the α-helical region (160–167) of the α2 domain, perhaps owing to multiple amino acid substitutions. The two helical turns are moved toward the long helix of the α1 domain, decreasing the width of the groove in this region by up to 2.4 Å.

The structure of the α3 domains of M3 and K^b are very similar, except for the exposed loop (195–197), connecting S1 to S2, and residues 222–227 on the surface, where main chain atoms deviate up to 2 Å. The 222–229 loop contains four highly conserved acidic residues, which may be important for electrostatic interactions with CD8 (Leahy et al., 1992). All four acidic residues are present in M3, and, in addition, Asn-220 and Gly-221 of K^b and D^b are replaced by acidic residues (aspartic acid and glutamic acid) in M3, which may therefore have higher affinity for CD8. T cell recognition of M3 is indeed CD8 dependent (Hermel, 1992).

Nonclassical Binding Sites for the Peptide Termini

M3 and K^b differ in 58 residues in the α1α2 domain. Of these, 20 form part of the molecular surface of the peptide-binding groove (Figure 2b). The most striking difference of the M3 groove is at the end of pocket A, where the peptide N-terminus resides in all other class I molecules. The change is primarily caused by the replacement of several side chains surrounding this region. In M3, consensus Trp-167 and Tyr-171 are replaced by leucine and phenylalanine. The side chain of Leu-167 in M3 points directly into the groove rather than upward, which dramatically decreases the size of pocket A (Figures 3a and 3b). Pocket A in the MHC class I–related neonatal Fc receptor, which does not bind peptides, is similarly occluded by the equivalent residue Arg-164 (Burmeister et al., 1994). Leu-167 also causes some rearrangement of side chains from neighboring residues. For example, the side chain of Arg-170, which forms a salt bridge with Glu-55, moves 4.4 Å into the groove and walls off the end. In addition, Glu-163 in M3 forms a salt bridge with Lys-66. Glu-163 is also present in D^b, but points out of the groove. The salt bridge across the groove limits peptide access further; the N-terminus of the MTF peptide does not extend into pocket A, but is instead located where P2 is found in other class I complexes. The replacement of consensus Val-34 by glutamine, whose side chain forms a hydrogen bond with the hydroxyl group of Tyr-59, may compensate for the loss of a hydrogen bond between Tyr-59 and Tyr-171, present in all other class I molecules.

Table 3. Hydrogen Bonds between β_2m and Heavy Chain of M3

β_2M	α1α2	K^b	A2	β_2m	α3	K^b	A2
H31 (NE2)	Q96 (OE1)	+	+	Q8 (NE2)	E232 (O)	−	+
D53 (OD2)	Q32 (NE2)	−	+	Q8 (OE1)	R234 (NH1)	+	+
D53 (OD1)	R35 (NH1)	−	+	Y10 (OH)	P235 (O)	+	+
D53 (OD2)	R48 (NE)	−	+	S11 (O)	Q242 (NE2)	+	+
D53 (OD1)	R48 (NH2)	−	+	R12 (NE)	S236 (O)	−	+
W60 (O)	Q96 (NE2)	+	+	R12 (O)	Q242 (NE2)	−	+
W60 (NE1)	D122 (OD1)	+	+	N24 (OD1)	S236 (O)	+	+
Y63 (OH)	Y27 (OH)	−	+	T28 (OG1)	E232 (OE2)	−	−
				Q29 (OE1)	E232 (OE2)	+	−
				D98 (O)	R202 (NE)	−	+
				M99 (O)	R234 (NH2)	−	+
				M99 (O)	R234 (NH1)	−	+
				M99 (O)	W244 (NE1)	−	+

Hydrogen bonds were assigned for donor–acceptor distances <3.4 Å. Interactions are marked by plus if also present and by minus if absent in K^b or A2.

The N-formyl group does not interact with any residue in pocket A. This explains why M3 mutants with consensus residues in pocket A (Val-34, Trp-167, or Tyr-171) can still present N-formylated peptides (Smith et al., 1994). Consistent with the report that P1 glycyl analogs of M3-binding peptides do not require N-formylation to bind (Vyas et al., 1992), our computer modeling suggested that such peptides can extend into pocket A with minimal adjustment of some M3 side chains and may form hydrogen bonds with Tyr-7 and Tyr-59. Any bulkier P1 side chain would be excluded from pocket A owing to steric hindrance from Leu-167 and Glu-163.

At the other end of the groove in M3, consensus Trp-147 is replaced by leucine, which also points into the groove but makes it more spacious. Lys-146 is replaced by arginine, which also forms a hydrogen bond with the hydroxyl group of Tyr-84 (Figure 3c). Relative to K^b, the aromatic ring of Tyr-84 and the side chain of Arg-146 are shifted up and outward in M3, allowing the C-terminus of the peptide to protrude from the M3 groove.

Binding Site for N-Formyl-Methionine

The most intriguing property of M3 is the specificity for N-formylated peptides. In the M3–MTF complex, the N-terminus of the peptide is located in the vicinity of residues Tyr-7, His-9, Val-99, and Tyr-159. The methionine side chain extends under the Lys-66–Glu-163 salt bridge into the deep pocket B, between the floor of the cleft and the α helix in the α1 domain. The formyl group is stabilized in a novel hydrogen bond network, including Tyr-7, His-9,

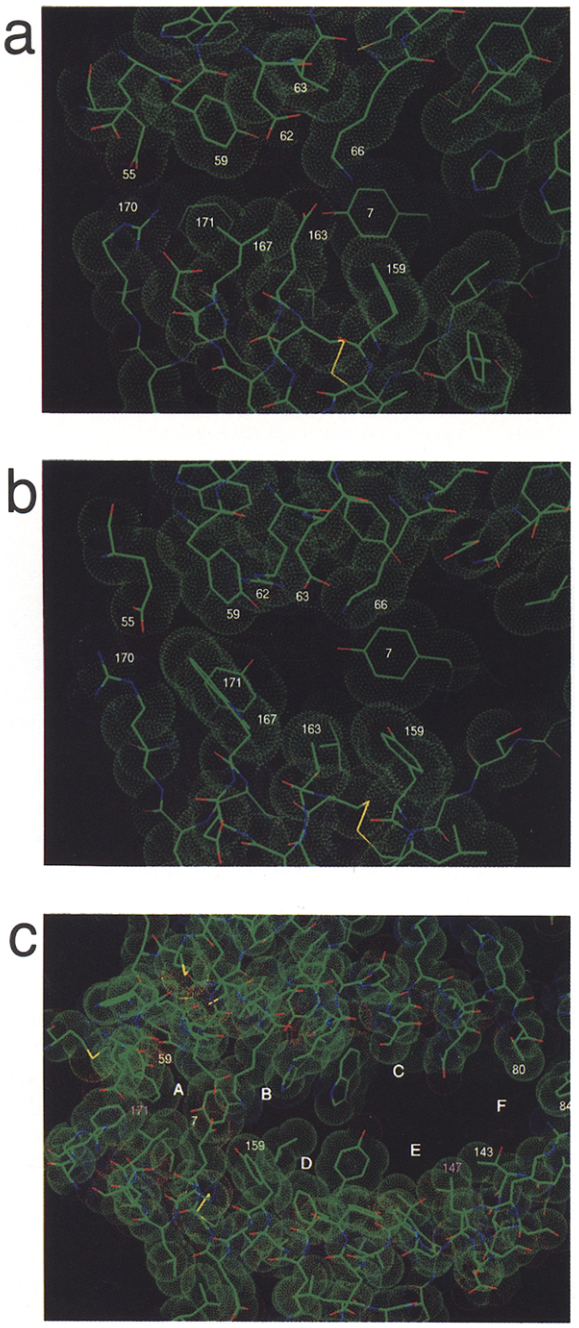

Figure 3. Van der Waals Surface of the Vicinity of Pocket A

(a and b) Van der Waals surface of the vicinity of pocket A in the peptide-binding groove of M3 (a) and the corresponding region of K^b (b). The surfaces are colored by atom type (carbon, green; nitrogen, blue; oxygen, red; sulphur, yellow).

(c) Molecular surface of pockets in the M3 peptide-binding groove, seen from above. Pockets A to F were assigned as in the A2 structure. Residues at the ends of the groove are labeled in white when conserved in all the MHC class I structures and in pink when unique to M3.

Tyr-159, Glu-163, and a water molecule (Wat1002) (Figure 4; Table 4). His-9 may play the most important role in the 10^4-fold preference of M3 for N-formylated peptides. It forms a hydrogen bond with the carbonyl oxygen of the

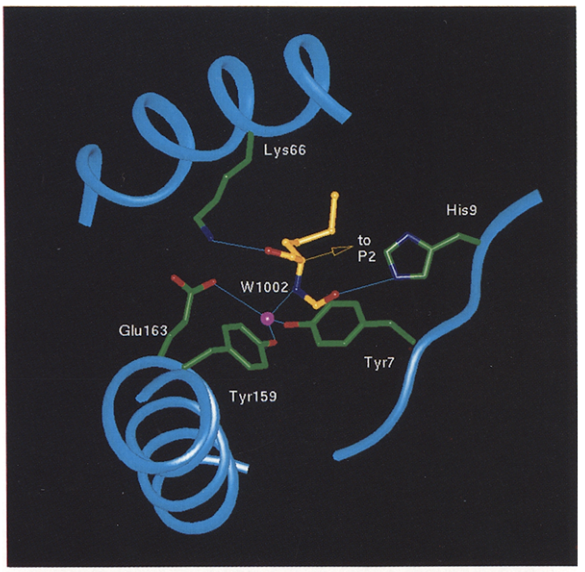

Figure 4. Hydrogen Bond Networks for MTF N-Terminus

Hydrogen bonds (blue lines) are formed by fMet (orange) to side chains (green) of M3 (Cα ribbon in cyan) and a water molecule (magenta). Nitrogens are blue and oxygens red. The view along the α2 α helix was chosen to show all hydrogen bonds.

formyl group, which would be missing for nonformylated peptides. In addition, it forms a second hydrogen bond with Tyr-22 and is in close contact with Trp-97. The interaction of His-9 with these aromatic residues can stabilize the protonated form of histidine and increase the pKa (Loewenthal et al., 1992); thus, it is likely that His-9 is positively charged at physiological pH, which will impede the binding of nonformylated peptides by charge repulsion. N-acetylated analogs of MTF peptides do not bind to M3 (Shawar et al., 1990), and computer modeling showed that changing the N-formyl to an N-acetyl group would cause steric interference with the aromatic ring of Tyr-7.

Structural Features of Peptide-Binding Groove

All six pockets identified in class Ia structures can be found in M3 at similar locations, but their size, shape, and chemical properties are unique to M3 (see Figure 3c). Pocket A in M3 is occluded and filled with two water molecules. Pocket B is spacious in M3, owing to the changed orientation of the Met-45 side chain, which points away from the groove in M3, and the smaller side chains Ser-24 and Cys-36 in M3 compared with glutamic acid and phenylalanine in K^b. The P1-Met side chain of MTF is completely buried in pocket B, and an ordered water molecule at the bottom forms hydrogen bonds with side chains of Gln-34 and Ser-24. Pocket B appears large enough to accommodate even bulkier side chains, such as tryptophan or arginine, if the water molecule is excluded; this is consistent with results from peptide-binding competition (Vyas et al., 1992). The pocket may be able to accommodate both hydrophobic and polar side chains, because its surface, though predominantly hydrophobic, has some polar patches; it is made up of Tyr-7, His-9, Tyr-22, Ser-24, Cys-36, Val-67, Ile-70, Val-99, and Tyr-159.

Table 4. Hydrogen Bonds and van der Waals Interactions between the MTF Peptide and M3

Peptide Residue[a]	Hydrogen Bonding[b] Atom	Partner	Van der Waals Contacts[c]
P1-fMet	OF	H9 (NE2)	Y7 (11), H9 (1), Y22 (1), S24 (1), L63 (1), K66 (1), V67 (1), I70 (2),
	N	Y159 (OH)	V99 (3), Y159 (6), Wat1002 (1), Wat1007 (1), Wat1189 (1)
		Wat1002	
	O	K66 (NZ)	
P2-Tyr	O	W97 (NE1)	H9 (1), I70 (1), W97 (1), V99 (1), Y155 (1), Y156 (1), Y159 (2)
P3-Phe		None	I70 (1), S73 (4), N77 (5), L95 (1), W97 (8), Wat1188 (1)
P4-Ile	N	Y114 (OH)	Y114 (3), L147 (2), T152 (2)
	O	Wat1188	
P5-Asn		None	N77 (2), L147 (1)
P6-Ile	N	N77 (OD1)	N77 (7), Y123 (2), T143 (2)
P7-Leu	N	N77 (OD1)	N77 (1), T80 (4), Y84 (3), Y123 (1), I142 (1), T143 (3), R146 (1)
P8-Thr	N	R146 (NH1)	T80 (1), Y84 (1), R146 (2)
	OG1	R146 (NH1)	

[a] The electron density of P9 was not defined sufficiently well to allow unambiguous assignment of interactions.
[b] Hydrogen bonds were assigned as in Table 3.
[c] Contacts of <4 Å between peptide and M3 are listed with their numbers in parentheses.

The location of pocket C differs significantly from K^b, owing to the change of Val-97 to tryptophan, which clearly defines the border to pocket B. As in A2, pocket C of M3 is located on the inner wall of the α1 helix above residue 74, surrounded by Ile-70, Ser-73, Asn-77, Trp-97, and Leu-95. The pocket is much larger than the comparable region in A2, owing to the change of His-74 to alanine. The P3-Phe side chain of MTF lodges in this pocket.

Pocket D in M3 is along the α2 domain α helix near residue 156. The side chains forming the pocket include four tyrosines, Tyr-114, Tyr-155, Tyr-156, and Tyr-159, which may confer affinity toward peptides with an aromatic side chain at P2; the surface of this pocket is entirely hydrophobic. Tyr-155 points upward instead of into the binding groove, making the pocket larger than in other class I molecules. The P2-Tyr side chain of MTF fits into this pocket. Screening of phage peptide display libraries with soluble M3 molecules yielded peptides of which 65% had an aromatic residue at P2 (Miller et al., 1994).

Pockets E and F are continuous in the M3 binding groove. Trp-147 and Tyr-116, which separate these pockets in other class I molecules, are replaced by the smaller side chains of Leu-147 and Ala-116. In K^b and A2, Trp-147 and Tyr-116 form hydrogen bonds with main chain atoms of bound peptides (Fremont et al., 1992; Madden et al., 1993). The loss of these hydrogen bonds in M3 and the increased size of the cavity, occupied by P4-Ile and P6-Ile, may allow more conformational freedom for the bound peptide; this may explain why the B factors for residues at this end of the peptide are higher than for peptides bound in other class I grooves.

Overall, the groove in M3 is narrower at the N-terminal end and wider and deeper at the C-terminal end, and the residues surrounding the pockets in M3 are predominantly hydrophobic (Figure 5a). MTF buries 692 $Å^2$ of the solvent accessible surface of M3, which is within the range of other class I–peptide complexes (671–772 $Å^2$). However, the surfaces buried by MTF have a significantly higher proportion (~70%) of nonpolar atoms than the total molecular surface of M3 (53%) or the surfaces buried in other class I–peptide complexes (49%–57%) (Figure 5b).

Peptide Conformation

Before inclusion of any peptide model in the refinement, continuous electron density was evident in the M3 groove. After refinement, the peptide electron density is clearest for the first three residues, which are buried deeply in the groove, and weakest for P8 and P9, which come out of the groove and are most exposed to the solvent. The backbone atoms of the first four peptide residues are closer to the floor of the groove than in other class I–peptide complexes, and the first seven residues have an extended backbone conformation (see Figure 1b). Because of the wide groove and the lack of extensive interactions, the C-terminal end of the peptide in M3 may adopt several slightly different conformations, as reflected by the high B factor. In the M3–MTF crystals, the grooves from the two molecules in the unit cell face each other. The conformation of the peptides in the two molecules are similar for the first seven residues, with an rmsd of Cα atoms of ~0.35 Å. The last two residues differ significantly between the molecules because the C-terminus of the peptide in molecule 2 is involved in a crystal contact with Arg-146 of molecule 1. The guanidinium group of Arg-146 in molecule 2 has shifted ~2 Å outward, and the hydroxyl group of Tyr-84 has moved 1.3 Å, allowing the C-terminus of MTF in molecule 2 to extend ~1 Å further along the groove. Nevertheless, the last residue of this peptide is still highly exposed to solvent. The C-terminal end of the groove in M3 thus appears quite flexible and able to adjust its conformation to accommodate longer peptides. Because the peptide conformation in molecule 2 is clearly influenced by crystal contacts, only molecule 1 was used to discuss the M3–peptide interactions.

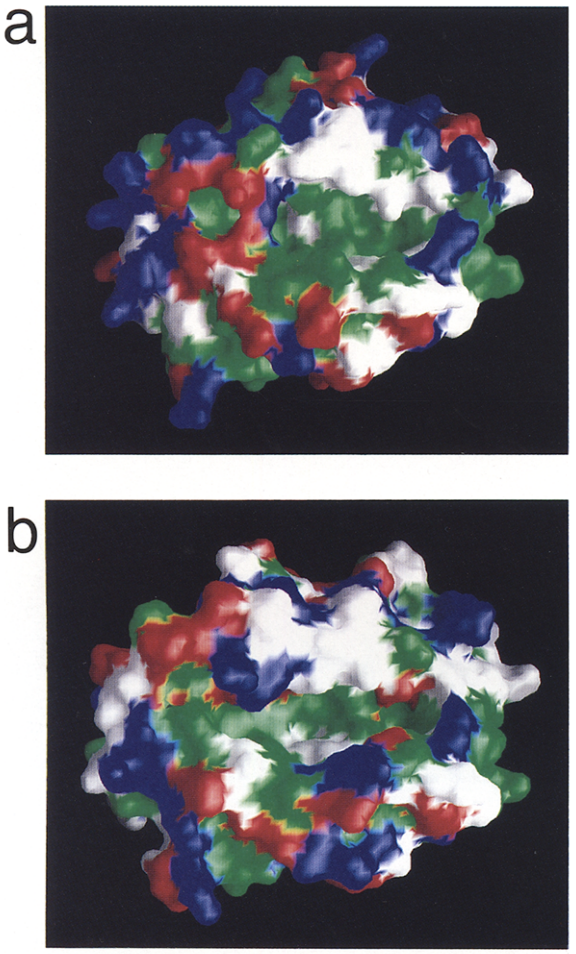

Figure 5. Hydrophobicity of Molecular Surfaces of the α1α2 Domains of M3 and K^b

Molecular surfaces of the α1α2 domains of M3 (a) and K^b (b), viewed from the top and displayed by color. Residues with nonpolar side chains (A, L, I, V, M, Y, F, and W) are green, residues with polar side chains (G, S, T, C, P, H, N, and Q) are white, aspartic acid and glutamic acid are red, and arginine and lysine are blue. The surfaces were calculated and displayed with the program GRASP (Nicholls et al., 1991).

Our choice of an MTF nonamer in the crystallization was based on the observation that most peptides extracted from class I molecules are nine (or, less frequently, eight) residues long (Rammensee et al., 1993). Because of the novel binding mode with the P1 side chain in pocket B, this nonamer is too long to fit, and the C-terminus of the peptide extends out of the groove. A similar extension from the C-terminal end of the groove was observed for a decamer peptide bound by A2 (Collins et al., 1994). Another way to accommodate longer peptides, observed in class Ia molecules, is by additional kinking of the peptide backbone near the center, such that the hydrogen bond interactions with both ends of the peptide-binding groove are maintained (Guo et al., 1992). Such bulging in the middle of the MTF peptides would be incompatible with the packing of the M3 crystals.

Peptide Interactions

Interactions between MTF and M3 are extensive, including 98 van der Waals contacts and nine hydrogen bonds. MTF makes two additional hydrogen bonds to water molecules, which in turn hydrogen bond to M3 (Table 4). As in class Ia structures, most hydrogen bonds are between side chains of M3 and the main chain of the peptide.

The degree of complementarity between the interacting surfaces of M3 and MTF was estimated by the shape correlation statistics, calculated with the program SHAPE (Lawrence and Colman, 1993), to be 0.68, which is similar to antigen–antibody interactions. The extensively interacting surfaces were in pockets B, C, D, and E as well as where the formyl group of the peptide bound (Figure 6). Of the solvent accessible surface of the peptide, 73% (993 Å²) is buried upon binding to M3 (Figure 7); 58% of the buried surfaces and 68% of the van der Waals contacts are contributed by the first four peptide residues, and the binding of these residues may be sufficient to hold a peptide in the groove (Vyas et al., 1995). This may explain why some chemotactic formyl peptides, such as fMLF, fMLFF, and fMLFK, can bind to M3, albeit with much lower affinities than MTF (Parner et al., 1992). The side chains of P2,

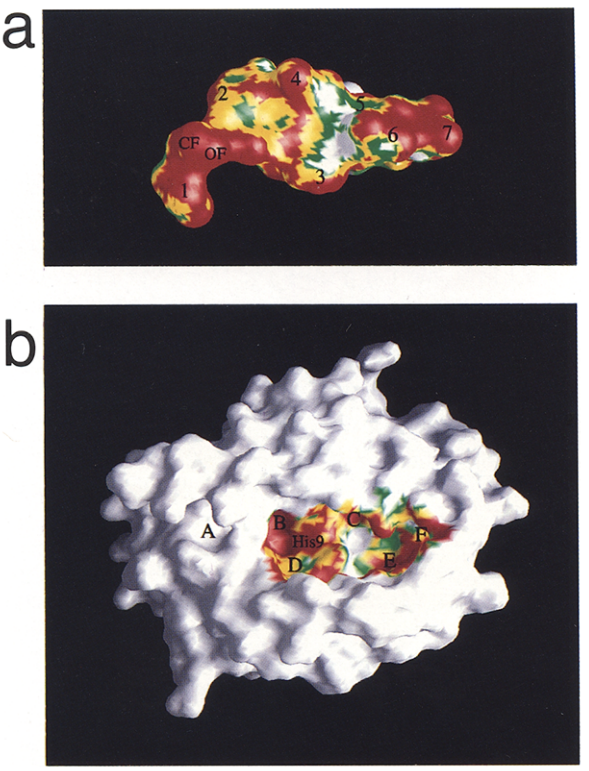

Figure 6. Interacting Surfaces of MTF and M3

Interacting surfaces of MTF (a), viewed from the bottom of the groove, and M3 (b), viewed from the top. Peptide residues are numbered, and the formyl group is marked by C and O. The degree of complementarity, color coded from highest (red) to lowest (white) over yellow and green, was calculated with the program SHAPE (Lawrence and Colman, 1993) and displayed with the program GRASP (Nicholls et al., 1991).

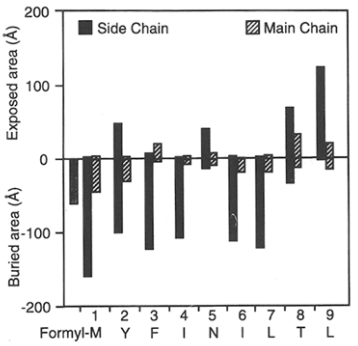

Figure 7. Solvent Accessible Surfaces of MTF Peptide

Negative values represent the surfaces buried by the interaction with M3; positive values represent the surfaces exposed to solvent.

P5, P8, and P9 of MTF are accessible to solvent and are therefore available for direct interactions with T cell receptors.

M3 Alleles and Homologs

Unlike class Ia molecules, M3 shows little polymorphism. The most interesting allelic form is $M3^{cas}$ (formerly HMT^{b}), to which we have been unable to raise an immune response. $M3^{wt}$ and $M3^{cas}$ differ in their α1α2 domain only by Val-31 to methionine and Leu-95 to glutamine substitutions in the *cas* form (Wang et al., 1991). Site-specific mutation of Leu-95 to glutamine eliminates T cell recognition of M3–peptide complexes, whereas mutation at position 31 has much less effect on recognition by bulk populations of killer T cells (Wang and Fischer Lindahl, 1993). This result is consistent with the structure of the M3–MTF complex. The side chain of Leu-95 points up from the β-sheet floor into the groove and forms van der Waals contacts with side chains of P3-Phe and P6-Ile. Change of Leu-95 to glutamine, with a larger and polar side chain, may affect binding affinity and conformation of the peptide and thereby its recognition by T cell receptors. Val-31 is in the loop between two β strands, and its side chain points toward the α3 domain, within van der Waals contact with Tyr-209; substitution with methionine might change the conformation of the α1 loop.

Because of its specialized function, it was of interest to search for M3 homologs in other species. An M3 ortholog, RT1.M3, is expressed in the rat (Wang et al., 1995), and residues that contribute to the specificity for formylated peptides, including His-9, Leu-167, Lys-66, and Glu-163, are conserved in RT1.M3. Hybridization with an *M3*-specific probe failed to detect orthologs in guinea pig, rabbit, cow, or human DNA (Wang et al., 1991), but this does not rule out the existence of a functional homolog. However, none of >200 class I sequences from mouse, rat, cat, rabbit, pig, cow, and primates had all the characteristic M3 substitutions in the A pocket. The M3 mode of binding formylated peptides may therefore be unique to murine rodents, and other species may have evolved different mechanisms, as in the neutrophil receptor for chemotactic formyl peptides (Murphy, 1994).

T Cell Recognition

The M3 structure presented here reveals a novel hydrogen bond network that stabilizes N-formylated peptides in a unique location, and it provides evidence that longer peptides can be accommodated in class I molecules by letting the C-terminus hang out. In our current model, the side chain of the polymorphic (isoleucine, alanine, valine, or threonine) sixth residue of MTF is buried in the F pocket of the peptide-binding groove, and yet P6 is the residue by which cytotoxic T cells distinguish allelic forms of this minor histocompatibility antigen (Loveland et al., 1990). Attempts to model the MTF peptide such that the P6 side chain pointed outward resulted in conformations that were less consistent with the X-ray data and energetically unfavorable. The polymorphism of P6 may affect T cell recognition by altering the conformation of neighboring residues in MTF or M3 that are directly exposed to the T cell receptor. Recent studies have demonstrated that changes in peptide residues that are buried in the groove (Fremont et al., 1995) can influence recognition of the MHC class I molecule by T cells and monoclonal antibodies (Chen et al., 1993; Hogquist et al., 1993; Rohren et al., 1994). Comparison of crystal structures of M3 complexed with different alleles of MTF may show how induced conformational changes can modulate T cell recognition of hidden residues.

Experimental Procedures

Construction and Expression of Soluble M3 Molecules

A truncated $M3^{wt}$ cDNA fragment (GenBank accession number U18797), which encodes the leader peptide (Met(−24)–Ser(−1)) and the α1α2α3 extracellular domains (Gly-1 to Trp-274), was amplified from the $M3^{wt}$ cDNA clone pCDM3 (Wang et al., 1991) by polymerase chain reaction with the oligonucleotides 5′-CCGAATTCACCATGGGGTCCTCAAGCAACTG-3′ and 5′-TCATAGGTACCAAGATCTCCATTTCAGGGCAAGGG-3′. The resulting fragment was digested with EcoRI and BglII and cloned into the modified version of expression vector pRMHa-3, which directs protein expression under the metallothionein promoter and incorporates a C-terminal His_6 tag to facilitate purification. The resulting M3 protein contained the three extracellular domains (residues 1–274) and eight additional amino acids (Arg–Ser–His_6) at the C-terminus. A full-length mouse $B2m^{a}$ cDNA cloned into pRMHa-3 has been described (Matsumura et al., 1992b). Drosophila S2/M3 cells were cotransfected with both expression plasmids and the phshsneo plasmid by the calcium–phosphate precipitation method, and stable transfectants were selected in medium containing G418 (0.5 mg/ml) as described previously (Matsumura et al., 1992b).

Purification and Crystallization of M3–MTF Complex

For production of secreted M3 molecules, 6 liters of stably transfected Drosophila cells were grown at 27°C in serum-free medium (Insect X-press, Bio-Wittaker) in rolling bottles. When the cell density reached ~4 × 10^6 cells/ml, cupric sulfate was added to a final concentration of 1 mM to induce expression, and the cultures were continued for another 3 days. Culture supernatants were collected by centrifugation and concentrated by membrane ultrafiltration (Millipore TFF cartridge, 30 kDa cutoff). Soluble M3 molecules in the supernatant were adsorbed onto a Ni–NTA (Qiagen) column at 4°C. The bound M3 molecules were eluted with 100 mM imidazole in phosphate-buffered saline (pH 7.4). The protein was purified further by ion exchange chromatography (Mono Q, Pharmacia) with a linear gradient of 0–300 mM NaCl in 50 mM Tris–HCl (pH 7.5). Typically, 0.5 mg of soluble M3 molecules was purified to homogeneity from 1 liter of culture medium. The purified M3 molecules were mixed with synthetic peptide corresponding to the rat MTF sequence (fMYFINILTL) (Hermel, 1992) in a molar ratio of 1:3. The mixture was incubated at room temperature for 4 hr and

then dialyzed overnight against 20 mM Tris–HCl (pH 7.5) at 4°C. The resulting complex was then concentrated to 6 mg/ml by ultrafiltration (Centricon 10, Amicon).

Crystals were grown by the sitting drop vapor diffusion method. The best crystals were obtained by mixing 4 μl of M3–MTF complex (6 mg/ml protein in 20 mM Tris–HCl [pH 7.5]) with an equal volume of crystallization well solution (16%–18% PEG 8000, 100 mM HEPES, 2% 2,4-methylpentanediol [pH 7.5]) at 26°C. The crystals grew over the course of 2 weeks to a final size of ~0.1 × 0.15 × 0.8 mm^3.

Data Collection and Molecular Replacement

X-ray diffraction data to 2.1 Å resolution were collected at 4°C from a single crystal with an RAXIS-II imaging plate area detector. Raw data were indexed, integrated, scaled, and merged with the programs DENZO and SCALEPACK, written and provided by Z. Otwinowski. The crystals have the symmetry of space group P1 with the unit cell dimensions a = 65.25 Å, b = 66.10 Å, c = 55.17 Å; α = 102.71°, β = 96.28°, γ = 110.19°; and two molecules per unit cell (50% solvent content). Crystals with different cell dimensions (a = 65.79 Å, b = 70.78 Å, c ≈ 55.42 Å; α = 101.56°, β = 94.79°, γ = 114.66°) were obtained under the same crystallization conditions but diffracted to only 2.5 Å.

The structure was determined by molecular replacement using K^b as a starting model (Fremont et al., 1992). The amino acids that differ from M3 were changed to alanine, and the VSV peptide was omitted. The rotation function, Patterson correlation refinement, and translation function were all calculated with the program X-PLOR (Brünger, 1992b). Reflections from 10 to 3.5 Å were used in the search. The two highest peaks in the rotation function (Eulerian angles of θ1 = 316.48°, θ2 = 75.48°, θ3 = 103.29°; and θ1 = 125.93°, θ2 = 92.36°, θ3 = 87.10°) are related by the rotation axis defined by the polar angles ψ = 84.05°, Φ = 174.69°, κ = 192.04°. These two peaks also produced the top two solutions after Patterson correlation refinement and were used in a translation search. A single clear solution (12σ) was obtained with the translation vector t = (5.09, 38.74, 28.36) Å between the two molecules in the unit cell.

Refinement and Model Building

The crystallographic refinement of M3 proceeded in five stages. Stage I was a rigid body refinement with data from 8 to 4 Å resolution, in which the α1α2, α3, and β_2m domains of each molecule were treated as separate. This reduced the R factor to 39.1%.

In stage II, we used data from 8 to 2.5 Å resolution to do simulated annealing refinement, followed by conjugate–gradient energy minimization. From stage II to the end of the refinement, we applied noncrystallographic symmetry restraints to atomic coordinates and B factors of all residues of M3 and β_2m, except those involved in crystal contacts. At the end of stage II, the R factor was 28%, and $2F_o–F_c$ electron density maps calculated with SIGMAA weights (Read, 1986) were readily interpretable for most of the residues, except in some loop regions. Disconnected pieces of electron density appeared in the peptide-binding groove. Model building and fitting of most of the M3-specific residues were done with the program O (Jones et al., 1991).

In stage III, we included data between 20 and 2.1 Å resolution, which increased the R factor by ~2%, although we performed a bulk solvent correction. Nevertheless, the inclusion of low resolution data substantially improved the connectivity of the electron density maps for the loops and the peptide. Each refinement cycle consisted of several steps of conjugate gradient minimization, with stepwise extension of the high resolution limit, restrained individual B-factor refinement, and model building. For the "free R" utility of X-PLOR (Brünger, 1992a), we reserved 10% of the data in a "test" set that was not used in the refinement. The R factor of the test set typically lagged behind that of the working set by 8%–10%. After five rounds of refinement and model building, the R factor dropped to 23.4% for 20–2.1 Å (21.8% for 6–2.1 Å data).

In stage IV, water molecules were added in an automatic process, placing them at peaks ≥3σ in an $F_o–F_c$ map only when those peaks fell near potential hydrogen bond acceptors/donors and did not collide with any other atoms. In four cycles of water addition, refinement, removal of waters with B factor >60 $Å^2$, and minor model building, a total of 352 water molecules were added. A carbohydrate moiety (N-acetyl-glucosamine) was also modeled into a flat, connected density extending from the amide group of Asn-86 in one of the M3 molecules. At this stage, the R factor was 20.7% for the working data set and 29.8% for the test set from 20 to 2.1 Å. The electron density was continuous for the peptide main chain along the groove and showed side chains of P1–P3.

Refinement stage V began with building of a heptamer peptide into the density. Because the electron density in the region corresponding to P4 and P5 was extensive but not well defined, the occupancies for the atoms in residues P4–P7 were set to zero. Simulated annealing refinement was carried out at 3000°K (Brünger et al., 1990), followed by conjugate–gradient energy minimization and restrained individual B-factor refinement; this improved the R factor 0.8% for the working data set and 0.4% for the test set. The electron density for the peptide was substantially improved: additional electron density corresponding to P7 and P8 appeared, and the side chain densities for P4, P5, and P6 became clearer. A nonamer peptide (fMYFINILAA) was built, and water molecules close to the peptide-binding site were picked manually and refined. Following refinement, the electron density was slightly improved for the side chains of P8 and P9. A complete MTF peptide (fMYFINILTL) was then built and refined, yielding an R factor of 19.0% for all the data with $F_o > 2\sigma(F_o)$ from 20 to 2.1 Å. Data previously in the test set were included in the last cycle of refinement. The mean coordinate error was estimated to be 0.28 Å based on a Luzzati plot (Luzzati, 1952) and 0.35 Å based on the SIGMAA method (Read, 1986).

Atomic coordinates have been deposited with the Brookhaven Protein Data Bank.

Acknowledgments

We thank Drs. Lothar Esser, Charles A. Hasemann, Ravi G. Kurumbail, Hee-Won Park, and Mr. San-Tai Shen for help and advice and Ms. Dorothee B. Staber for assistance with the manuscript.

Received May 9, 1995; revised June 29, 1995.

References

Aldrich, C. J., DeCloux, A., Woods, A. S., Cotter, R. J., Soloski, M. J., and Forman, J. (1994). Identification of a Tap-dependent leader peptide recognized by alloreactive T cells specific for a class Ib antigen. Cell *79*, 649–658

Bjorkman, P. J., Saper, M. A., Samraoui, B., Bennett, W. S., Strominger, J. L., and Wiley, D. C. (1987a). The foreign antigen binding site and T cell recognition regions of class I histocompatibility antigens. Nature *329*, 512–515.

Bjorkman, P. J., Saper, M. A., Samraoui, B., Bennett, W. S., Strominger, J. L., and Wiley, D. C. (1987b). Structure of the human class I histocompatibility antigen, HLA-A2. Nature *329*, 506–512.

Brünger, A. T. (1992a). Free R value: a novel statistical quantity for assessing the accuracy of crystal structures. Nature *355*, 472–475.

Brünger, A. T. (1992b). X-PLOR Manual Version 3.0: A System for Crystallography and NMR (New Haven, Connecticut: Yale University Department of Molecular Biophysics and Biochemistry).

Brünger, A. T., Krukowski, A., and Erickson, J. (1990). Slow-cooling protocols for crystallographic refinement by simulated annealing. Acta Crystallogr. *A46*, 585–593.

Burmeister, W. P., Gastinel, L. N., Simister, N. E., Blum, M. L., and Bjorkman, P. J. (1994). Crystal structure at 2.2 Å resolution of the MHC-related neonatal Fc receptor. Nature *372*, 336–343.

Castaño, A. R., Tangri, S., Miller, J. E. W., Holcombe, H., Jackson, M. R., Huse, W. D., Kronenberg, M., and Peterson, P. A. (1995). Peptide binding and presentation by mouse CD1. Science *269*, 223–226.

Chen, W., McCluskey, J., Rodda, S., and Carbone, F. R. (1993). Changes at peptide residues buried in the major histocompatibility complex (MHC) class I binding cleft influence T cell recognition: a possible role for indirect conformational alterations in the MHC class I or bound peptide in determining T cell recognition. J. Exp. Med. *177*, 869–873.

Collins, E. J., Garboczi, D. N., and Wiley, D. C. (1994). Three-dimensional structure of a peptide extending from one end of a class I MHC binding site. Nature *371*, 626–629.

Fremont, D. H., Matsumura, M., Stura, E. A., Peterson, P. A., and Wilson, I. A. (1992). Crystal structures of two viral peptides in complex with murine MHC class I H-2K^b. Science *257*, 919–927.

Fremont, D. H., Stura, E. A., Matsumura, M., Peterson, P. A., and Wilson, I.A. (1995). Crystal structure of an H-2K^b-ovalbumin peptide complex reveals the interplay of primary and secondary anchor positions in the major histocompatibility complex binding groove. Proc. Natl. Acad. Sci. USA *92*, 2479–2483.

Garrett, T. P. J., Saper, M. A., Bjorkman, P. J., Strominger, J. L., and Wiley, D. C. (1989). Specificity pockets for the side chains of peptide antigens in HLA-Aw68. Nature *342*, 692–696.

Guo, H.-C., Jardetzky, T. S., Garrett, T. P. J., Lane, W. S., Strominger, J. L., and Wiley, D. C. (1992). Different length peptides bind to HLA-Aw68 similarly at their ends but bulge out in the middle. Nature *360*, 364–366.

Guo, H.-C., Madden, D. R., Silver, M. L., Jardetzky, T. S., Gorga, J. C., Strominger, J. L., and Wiley, D. C. (1993). Comparison of the P2 specificity pocket in three human histocompatibility antigens: HLA-A*6801, HLA-A*0201, and HLA-B*2705. Proc. Natl. Acad. Sci. USA *90*, 8053–8057.

Hermel, E. (1992). Characterization of ligands presented by medial class I histocompatibility antigens. PhD thesis, University of Texas Southwestern Graduate School, Dallas, Texas.

Hogquist, K. A., Grandea, A. G., III, and Bevan, M. J. (1993). Peptide variants reveal how antibodies recognize major histocompatibility complex class I. Eur. J. Immunol. *23*, 3028–3036.

Jackson, M. R., Song, E. S., Yang, Y., and Peterson, P. A. (1992). Empty and peptide-containing conformers of class I major histocompatibility complex molecules expressed in *Drosophila melanogaster* cells. Proc. Natl. Acad. Sci. USA *89*, 12117–12121.

Jones, T. A., Zou, J.-Y., Cowan, S. W., and Kjeldgaard, M. (1991). Improved methods for building protein models in electron density maps and the location of errors in these models. Acta Crystallogr. *A47*, 110–119.

Joyce, S., Tabaczewski, P., Angeletti, R. H., Nathenson, S. G., and Stroynowski, I. (1994). A non-polymorphic MHC class Ib molecule binds a large array of diverse self peptides. J. Exp. Med. *179*, 579–588.

Kurlander, R. J., Shawar, S. M., Brown, M. L., and Rich, R. R. (1992). Specialized role for a murine class I-b MHC molecule in prokaryotic host defenses. Science *257*, 678–679.

Lawrence, M. C., and Colman, P. M. (1993). Shape complementarity at protein/protein interfaces. J. Mol. Biol. *234*, 946–950.

Leahy, D. J., Axel, R., and Hendrickson, W. A. (1992). Crystal structure of a soluble form of the human T cell coreceptor CD8 at 2.6 Å resolution. Cell *68*, 1145–1162.

Loewenthal, R., Sancho, J., and Fersht, A. R. (1992). Histidine-aromatic interactions in barnase: elevation of histidine pK_a and contribution to protein stability. J. Mol. Biol. *224*, 759–770.

Loveland, B. E., Wang, C.-R., Yonekawa, H., Hermel, E., and Fischer Lindahl, K. (1990). Maternally transmitted histocompatibility antigen of mice: a hydrophobic peptide of a mitochondrially encoded protein. Cell *60*, 971–980.

Luzzati, A. (1952). Traitement statistique des erreurs dans la determination des structures cristallines. Acta Crystallogr. *5*, 802–810.

Madden, D. R., Gorga, J. C., Strominger, J. L., and Wiley, D. C. (1991). The structure of HLA-B27 reveals nonamer self-peptides bound in an extended conformation. Nature *353*, 321–325.

Madden, D. R., Gorga, J. C., Strominger, J. L., and Wiley, D. C. (1992). The three-dimensional structure of HLA-B27 at 2.1 Å resolution suggests a general mechanism for tight peptide binding to MHC. Cell *70*, 1035–1048.

Madden, D. R., Garboczi, D. N., and Wiley, D. C. (1993). The antigenic identity of peptide–MHC complexes: a comparison of the conformations of five viral peptides presented by HLA-A2. Cell *75*, 693–708.

Matsumura, M., Fremont, D. H., Peterson, P. A., and Wilson, I. A. (1992a). Emerging principles for the recognition of peptide antigens by MHC class I molecules. Science *257*, 927–934.

Matsumura, M., Saito, Y., Jackson, M. R., Song, E. S., and Peterson, P. A. (1992b). *In vitro* peptide binding to soluble empty class I major histocompatibility complex molecules isolated from transfected *Drosophila melanogaster* cells. J. Biol. Chem. *267*, 23589–23595.

Miller, J. E. W., Haaparanta, T., Brunmark, A., Castaño, A. R., Peterson, P. A., and Huse, W. D. (1994). Rapid determination of class I peptide binding motifs using codon-based random peptide phage display libraries. J. Cell Biochem. (Suppl.) *18D*, 292.

Murphy, P. M. (1994). The molecular biology of leukocyte chemoattractant receptors. Annu. Rev. Immunol. *12*, 593–633.

Nicholls, A., Sharp, K., and Honig, B. (1991). Protein folding and association: insights from the interfacial and thermodynamic properties of hydrocarbons. Protein *11*, 281–296.

Pamer, E. G., Wang, C.-R., Flaherty, L., Fischer Lindahl, K., and Bevan, M.J. (1992). H-2M3 presents a Listeria monocytogenes peptide to CD8$^+$ cytotoxic T lymphocytes. Cell *70*, 215–223.

Rammensee, H.-G., Falk, K., and Rötzschke, O. (1993). Peptides naturally presented by MHC class I molecules. Annu. Rev. Immunol. *11*, 213–245.

Read, R. J. (1986). Improved Fourier coefficients for maps using phases from partial structures with errors. Acta Crystallogr. *A42*, 140–149.

Rohren, E. M., McCormick, D. J., and Pease, L. R. (1994). Peptide-induced conformational changes in class I molecules: direct detection by flow cytometry. J. Immunol. *152*, 5337–5343.

Rötzschke, O., Falk, K., Stefanovic, S., Grahovac, B., Soloski, M. J., Jung, G., and Rammensee, H.-G. (1993). Qa-2 molecules are peptide receptors of higher stringency than ordinary class I molecules. Nature *361*, 642–644.

Saper, M. A., Bjorkman, P. J., and Wiley, D. C. (1991). Refined structure of the human histocompatibility antigen HLA-A2 at 2.6 Å resolution. J. Mol. Biol. *219*, 277–319.

Shawar, S. M., Cook, R. G., Rodgers, J. R., and Rich, R. R. (1990). Specialized functions of MHC class I molecules. I. An N-formyl peptide receptor is required for construction of the class I antigen Mta. J. Exp. Med. *171*, 897–912.

Silver, M. L., Guo, H.-C., Strominger, J. L., and Wiley, D. C. (1992). Atomic structure of a human MHC molecule presenting an influenza virus peptide. Nature *360*, 367–369.

Smith, G. P., Dabhi, V. M., Pamer, E. G., and Fischer Lindahl, K. (1994). Peptide presentation by the MHC class Ib molecule, H2-M3. Int. Immunol. *6*, 1917–1926.

Stroynowski, I., and Fischer Lindahl, K. (1994). Antigen presentation by nonclassical class I molecules. Curr. Opin. Immunol. *6*, 38–44.

Vyas, J. M., Shawar, S. M., Rodgers, J. R., Cook, R. G., and Rich, R. R. (1992). Biochemical specificity of H-2M3^a: stereospecificity and space-filling requirement at position one maintains N-formyl peptide binding. J. Immunol. *149*, 3605–3611.

Vyas, J. M., Rodgers, J. R., and Rich, R. R. (1995). H-2M3^a violates the paradigm for MHC class I peptide binding. J. Exp. Med. *181*, 1817–1825.

Wang, C.-R., and Fischer Lindahl, K. (1993). HMT, encoded by *H-2M3*, is a neoclassical major histocompatibility class I antigen. Proc. Natl. Acad. Sci. USA *90*, 2784–2788.

Wang, C.-R., Loveland, B. E., and Fischer Lindahl, K. (1991). *H-2M3* encodes the MHC class I molecule presenting the maternally transmitted antigen of the mouse. Cell *66*, 335–345.

Wang, C.-R., Lambracht, D., Wonigeit, K., Howard, J. C., and Fischer Lindahl, K. (1995). Rat RT1 orthologs of mouse H2-M class Ib genes. Immunogenetics *42*, 63–67.

Young, A. C. M., Zhang, W., Sacchettini, J. C., and Nathenson, S. G. (1994). The three-dimensional structure of H-2D^b at 2.4 Å resolution: implications for antigen-determinant selection. Cell *76*, 39–50.

Zhang, W., Young, A. C. M., Imarai, M., Nathenson, S. G., and Sacchettini, J. C. (1992). Crystal structure of the major histocompatibility complex class I H-2K^b molecule containing a single viral peptide: implications for peptide binding and T-cell receptor recognition. Proc. Natl. Acad. Sci. USA *89*, 8403–8407.